A Theoretical Investigation of the Donor Ability of [M(R,R′timdt)₂] Dithiolene Complexes towards Molecular Diiodine (M = Ni, Pd, Pt; R,R′timdt = Formally Monoreduced Disubstituted Imidazolidine-2,4,5-trithione)

M. Carla Aragoni,[a] Massimiliano Arca,*[a] Francesco Demartin,[b] Francesco A. Devillanova,[a] Francesco Lelj,[c] Francesco Isaia,[a] Vito Lippolis,[a] Annalisa Mancini,[a] Luca Pala,[a] and Gaetano Verani[a]

The σ-type charge-transfer (CT) interaction between [M(R,R′timdt)₂] donors (M = Ni, Pd, Pt; R,R′timdt = formally monoreduced disubstituted imidazolidine-2,4,5-trithione) and diiodine has been thoroughly investigated by a large set of theoretical calculations at different levels of theory (HF, pure and hybrid-DFT with different functionals and basis sets) on I_2 (and for the sake of comparison on IBr and Br_2), on the model donor dithiolene complexes [M(H₂timdt)₂], and on the adducts [M(H₂timdt)₂]·I_2 (M = Ni, Pd, Pt). The computations have accounted for the ability of adducts to assume different stoichiometries and to make up polymeric networks based on sulfur–iodine contacts, as in the case of [Ni(Me,iPr-timdt)₂]·I_2, which was also characterised by single-crystal X-ray diffraction. In addition, the strength of the donor–acceptor interaction has been evaluated through the calculated vibrational features of the model adducts, compared with the experimental FT-Raman spectra recorded on the adducts between [M(Et₂timdt)₂] and [M(Me,iPr-timdt)₂] (M = Ni, Pd, Pt) and diiodine. The frontier-orbital composition, the NBO-charge distribution and bond orders indicate a medium-weak donor ability for the dithiolene donors, which depends only slightly on the nature of the central metal ion, and decreases on passing from M = Ni to M = Pd and Pt, in agreement with the values of the experimental frequencies of the FT-Raman-active I–I stretching vibrations in the adducts [M(Et₂timdt)₂]·$2I_2$ (M = Ni, Pd, Pt). The ZPE- and CP BSSE-corrected binding energy for [Ni(H₂timdt)₂]·I_2 has been evaluated as −11 kcal/mol.

(© Wiley-VCH Verlag GmbH & Co. KGaA, 69451 Weinheim, Germany, 2004)

Introduction

Since the pioneering work by Schrauzer and co-workers,[1] the scientific community has become increasingly interested in metal dithiolene complexes.[2] This is justified not only by the essential role of dithiolene ligands in the chemistry of enzymes[3−5] and by the great potential for exploiting these complexes in fields as diverse as nonlinear optics[6,7] and superconductivity,[8] but also by their fascinating electronic structures.[9] In particular, dithiolene complexes containing d^8 metal ions (namely Ni, Pd, and Pt) feature an extended π-electron delocalization involving the organic framework as well as the metal centre.[10] The electronic features are reflected in peculiar molecular properties, such as high thermal and photochemical stabilities, electrochromism,[10] and the ability to undergo multi-step reversible redox processes.[11,12] Square-planar neutral bisdithiolenes feature a peculiar very intense Vis/NIR absorption, which falls at 720, 785, and 680 nm for the simplest [M(edt)₂] neutral complexes [edt = ethylenedithiolato; M = Ni (**1**), Pd (**2**), and Pt (**3**), respectively].[1,13] This absorption has been ascribed to a HOMO−LUMO π-π* transition, based on theoretical calculations carried out at several levels of theory, ranging from EHT to TD-DFT.[14,15] The donor ability of the ligand towards the metal centre is tunable through structural modifications of the substituents at the carbon atoms of the dithiolene system, and affects both the Vis/NIR optical properties and the order of the relative stabilities of the available oxidation states (typically dianionic, monoanionic, and neutral).

Since 1995 we have been investigating neutral Ni, Pd, and Pt dithiolene complexes derived from the R,R′timdt ligand (R,R′timdt = formally monoreduced disubstituted imid-
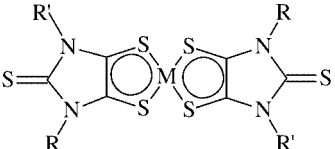
[a] Dipartimento di Chimica Inorganica ed Analitica, Università degli Studi di Cagliari,
S.S. 554 Bivio per Sestu, 09042 Monserrato − Cagliari, Italy
Fax: +39-070-6754456
E-mail: marca@unica.it
[b] Dipartimento di Chimica Strutturale e Stereochimica Inorganica, Università degli Studi di Milano,
Via G. Venezian 21, 20133 Milano, Italy
[c] LAMI Dipartimento di Chimica e LASCAMM-INSTM Sezione Basilicata, Università degli Studi della Basilicata,
Via N. Sauro 85, 85100 Potenza, Italy
Supporting information for this article is available on the WWW under http://www.eurjic.org or from the author.

azolidine-2,4,5-trithione), which differs from the very well-known dmit dithiolenes [dmit = $C_3S_5^{2-}$, 1,3-dithiole-2-thione-4,5-dithiolate;[8] M = Ni (**4**), Pd (**5**), Pt (**6**)] in having NR groups instead of sulfurs in the pentaatomic ligand (Scheme 1).[16–24] Hybrid-DFT[18,19,23] and very recent TD-DFT calculations[21,24] confirmed that the tight HOMO–LUMO energy gap is responsible for the low-energy NIR transition falling at about 1000 nm (extinction coefficients as high as 120000 $M^{-1}\cdot cm^{-1}$ in toluene).[23] In addition, contrary to most dithiolene complexes, and in particular to their dmit analogues, neutral [M(R,R′timdt)$_2$] complexes behave as donors towards molecular acceptors, and some of the authors of this paper have reported the reaction between [Ni(iPr$_2$timdt)$_2$] (**7**) and molecular diiodine, leading to the CT adducts **7**·2I$_2$ and **7**·2I$_2$·1/2I$_2$, and to the mixed-valence complex [Ni(iPr$_2$timdt)$_2$]·2I$_2$·[Ni(I)$_2$(iPr$_2$timdt)$_2$]·3I$_2$.[17] Among Pd complexes, only the CT adduct **8**·I$_2$·CHCl$_3$ (**8** = [Pd(Et$_2$timdt)$_2$]) has been reported,[18] while the reactivity of Pt dithiolene complexes towards diiodine has not been explored to date. In order to rationalize the donor ability of neutral [M(R,R′timdt)$_2$] complexes, we have now carried out a study on the products of the reactions between [M(Et$_2$timdt)$_2$] and [M(Me,iPr-timdt)$_2$] (M = Ni, Pd, Pt) and molecular I$_2$ in several molar ratios (Scheme 1).

R	R′	M	Dithiolene:I$_2$ reaction ratio			
			1:1	1:2	1:5	1:10
Et	Et	Ni	1:1	1:2	1:2	1:3
		Pd	2:1	2:1	1:2	1:2
		Pt	1:1	1:1	2:3	1:2
Me	i-Pr	Ni	1:1	1:1	1:1	1:4
		Pd	2:5	1:2	1:2	1:2
		Pt	1:3	1:4	1:5	1:5

Scheme 1

Theoretical calculations have recently been proved to be a very valuable tool in interpreting the interactions between chalcogenone donors and molecular halogens,[25] although it seems that the number of papers on complexes containing iodine is limited. Thus, with the aim of understanding the nature of the CT interaction and investigating the effect of the central metal ion and of the substituents on the reactivity of the metal dithiolene complexes [M(R,R′timdt)$_2$] towards molecular diiodine, we performed a large set of theoretical calculations on [M(H$_2$timdt)$_2$]·I$_2$ model adducts.

Results and Discussion

Synthesis

Since the low solubility of neutral [M(R,R′timdt)$_2$] complexes prevents them from reaching the concentrations needed to study their equilibria with iodine in solution,[26] neutral [M(R,R′timdt)$_2$] complexes (M = Ni, Pd, Pt), both symmetrically (R = R′ = Et) and unsymmetrically (R = Me; R′ = iPr) substituted, were reacted with molecular iodine in closed pressure-tubes (to avoid halogen losses) in dithiolene/iodine molar ratios ranging between 1:1 and 1:10, in order to achieve CT adducts with different stoichiometries. Unfortunately, conventional solid-state spectroscopic techniques (such as FT-Raman, FT-IR, and CP MAS ^{13}C NMR) are not useful in clarifying the nature of the final products, which can be only ascertained by elemental analysis and, when possible, by X-ray diffraction. Although the composition of the final products cannot be ascertained clearly in all cases (especially when R = Me, R′ = iPr), an examination of the dithiolene/I$_2$ molar ratios in the adducts (Scheme 1) shows that the halogen content in the final products increases on increasing the starting molar ratio, and that the nature both of the central metal and of the substituents is crucial in determining the final product. It is worthy of note that all the Pt complexes were found to react with I$_2$ yielding reaction products with dithiolene/halogen ratios ranging between 1:0.5 and 1:5 depending on the substituents. The isolation of several adducts with dithiolene/I$_2$ ratios higher than 1:2 suggests that the terminal iodine units of [M(R,R′timdt)$_2$]·2I$_2$ adducts should be able to behave as donors towards further diiodine molecules.

X-ray Diffraction Studies

Crystals having a 1:1 dithiolene/I$_2$ ratio, suitable for X-ray diffraction studies, were obtained by reacting [Ni(Me,-iPr-timdt)$_2$] (**9**) and I$_2$ in molar ratios ranging between 1:1 and 1:5. A perspective view of the 1:1 CT adduct **9**·I$_2$ is depicted in Figure 1. The nickel atom of the [Ni(Me,iPr-timdt)$_2$] molecule is located on a crystallographic inversion centre at 0,0,0 whereas the diiodine molecule lies across a different crystallographic centre at 0, 1/2, 1/2. As expected based on the few previously reported structures of CT adducts between [M(R,R′timdt)$_2$] complexes and diiodine,[17,18] the dithiolene coordinates the iodine molecule through its terminal thiocarbonyl groups with an S(3)···I(1) interaction of 3.098(2) Å. A view of the crystal packing of **9**·I$_2$ (Figure 2) shows the polymeric nature of the adduct. The packing consists of zig-zag polymeric chains made up of complex molecules symmetrically linked by iodine units bridging the terminal sulfur atoms [S(3)] of different molecules. The diiodine moieties are essentially perpendicular to the dithiolene molecular plane and the S(3)···I(1)−I(1)′′···S(3)′′ system is linear. Similar S···I−I···S systems have been isolated in several CT adducts between thioether macrocycles and diiodine.[27] In these systems, which structurally recall the I$_4^{2-}$ anion ($^-$I···I−I···I$^-$),[28]

the bridging iodine molecule is less elongated than in the corresponding 1:1 CT adducts. Chains of alternating dithiolene and diiodine units are packed by dithiolene stacking interactions analogous to those described for **9**,[19] with the nickel atom sandwiched between two imidazolidine rings of parallel adjacent dithiolene molecules, the distances between each nickel ion and the imidazolidine centroid being 3.72 and 3.77 Å in **9** and **9·I₂**, respectively. A comparison with the crystal structure of **9**[19] shows that the terminal thiocarbonyl group involved in the CT interaction is slightly elongated with respect to the free donor [C(3)−S(3) = 1.644(5) in **9**, 1.674(6) Å in **9·I₂**], in agreement with the situation generally found for CT adducts between thiocarboxyl donors and iodine.[29] However, this lengthening is small and is compatible with a weak sulfur−iodine interaction. The rest of the complex molecule displays bond lengths and angles close to those found in complex **9** [C(1)−C(2), C(1)−S(1), and C(2)−S(2) 1.396(6), 1.682(5), and 1.681(5) Å in **9**; 1.380(7), 1.719(6), and 1.688(5) Å in **9·I₂**]. Due to the bridging role of the halogen in **9·I₂**, the interaction between the metal complex and the diiodine units [S(3)···I 3.098(2) Å] is weaker than that observed in the case of either **7·2I₂·1/2I₂** [2.825(6) Å] or **8·I₂·CHCl₃** [2.815(3) Å].[17,18] Accordingly, the elongation of the I−I distance due to the CT interaction [2.790(1) Å in **9·I₂**; I−I = 2.715

Å for iodine in the solid state][30] is less than that found for the adducts **7·2I₂·1/2I₂** and **8·I₂·CHCl₃** [I−I distances 2.815(3) and 2.811(2) Å, respectively].

FT-Raman Spectroscopy

Because of the resonance Raman effect with the broad NIR absorption at about 1000 nm, the FT-Raman spectra of neutral [M(R,R′timdt)₂] complexes recorded with spectrometers based on a Nd:YAG laser (λ_{exc} = 1064 nm) allow us to identify the vibrations due to the MS₄ system.[19] The spectra show only two very intense peaks in the 500−50 cm⁻¹ region. The former falls at average values of 435, 427, and 425 cm⁻¹ for the Ni, Pd, and Pt complexes, respectively; the latter, which falls at 380 and 340 cm⁻¹ for the Ni and Pd complexes, respectively, was not observed for the Pt complex.[19] These peaks have been attributed to the a_g or b_{1g} bending and to the a_g stretching modes of the MS₄C₄ dithiolene system, respectively.[19,24] Analogous peaks also appear in the solid-state FT-Raman spectra of the synthesized CT adducts at frequencies very close to those recorded for the starting dithiolenes. In weak and medium-weak CT adducts, the lengthening of the inter-iodine bond length due to the CT interaction has been correlated to the lowering of the corresponding stretching vibration, which occurs at 180 cm⁻¹ for solid iodine, and is shifted towards lower frequencies in CT adducts (140−180 cm⁻¹).[29,31] Unfortunately, when using Nd:YAG FT-Raman spectrometers, the Raman enhancement of the metal-sulfur vibrations makes the peaks due to the I−I stretching mode barely visible. Nonetheless, in the cases of the adducts of the complexes [M(Et₂timdt)₂] (M = Ni, Pd, Pt), the peak due to the I−I stretching mode is clearly visible at 139,[32] 153, and 155 cm⁻¹, for M = Ni, Pd, and Pt, respectively (see Figure 3 for [M(Et₂timdt)₂]·2I₂ adducts). The position of the peaks indicates a medium-weak interaction between [M(R,R′timdt)₂] and I₂, whose strength decreases on passing from Ni to Pt. Unfortunately, the peak due to the I−I vibration is completely absent in the adducts of [M(Me,iPr-timdt)₂] dithiolenes.
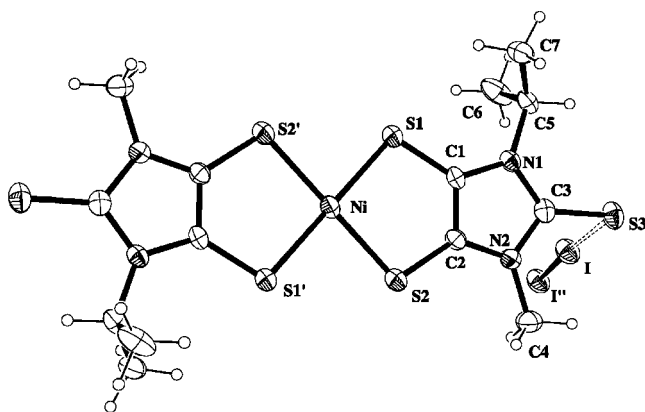

Figure 1. ORTEP structure and atom labelling scheme of **9·I₂**; selected bond lengths (Å): Ni−S(1), 2.176(2); Ni−S(2), 2.170(2); C(1)−S(1), 1.719(6); C(2)−S(2), 1.688(5); C(1)−C(2), 1.380(7); C(1)−N(1), 1.379(7); C(2)−N(2), 1.370(7); N(1)−C(3), 1.376(7); N(2)−C(3), 1.391(6); C(3)−S(3), 1.674(6); S(3)···I, 3.098(2); I−I′′, 2.790(1); selected angles (°): S(1)−Ni−S(2), 94.26(5); S(1)−Ni−S(2)′, 85.74(6); Ni−S(1)−C(1), 101.2(2); Ni−S(2)−C(2), 100.5(2); C(3)−S(3)···I(1), 93.26(8); S(3)···I−I′′, 176.27 (5); symmetry codes: ′ = −x, −y, −z; ′′ −x, 1 − y, 1 − z
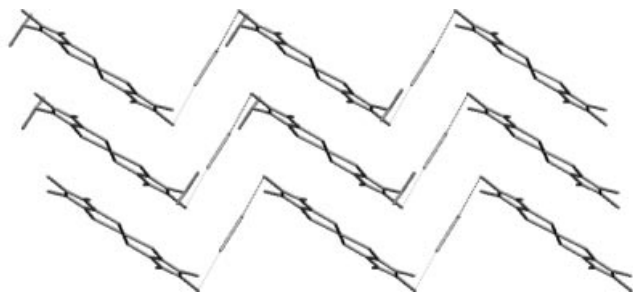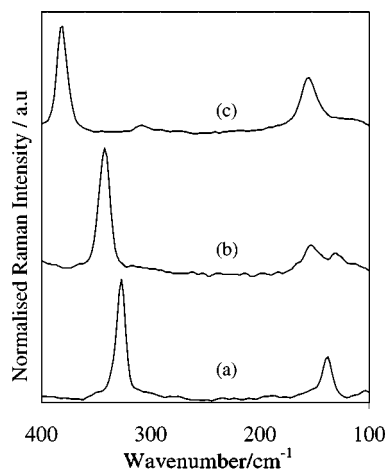

Figure 2. View of the crystal packing of **9·I₂**

Figure 3. Normalised FT-Raman spectra of the adducts [M(Et₂timdt)₂]·2I₂ [M = Ni (a), Pd (b), Pt (c)]

Theoretical Calculations

A few years ago, we reported[18,19,23] DFT[33,34] calculations performed with the Gaussian 98 package[35] on [M(H$_2$timdt)$_2$] model complexes [M = Ni (**10**), Pd (**11**), Pt (**12**); R = R′ = H in Scheme 1] using the three-parameter[36] hybrid B3LYP functional (based on the gradient-corrected Becke exchange functional[37] along with the Lee, Yang and Parr correlation functional[38]), and the LanL2DZ basis set (BS) with Effective Core Potentials (ECP)[39] for the central metal ion. With the results of these calculations it was possible to explain the trend in the NIR absorption maxima experimentally found on changing the central metal ion [λ_{max} (Ni) ≈ λ_{max} (Pt) < λ_{max} (Pd)], and the electrochemical behaviour of [M(R,R′timdt)$_2$] complexes compared to other neutral dithiolenes, such as **1**−**3** and **4**−**6**. In fact, TD-DFT calculations showed that the NIR excitation energy is well-represented by an almost pure HOMO−LUMO transition.[21,24] It has been proved that Kohn−Sham (KS) one-electron energies −ε of occupied orbitals can be interpreted as approximate relaxed vertical ionisation potentials.[40] Thus, the energy of the NIR transition can be estimated as the one-electron energy difference $\Delta\varepsilon$ between the HOMO and the LUMO.[18,19,21,23,24] At any rate, although the previous calculations accounted nicely for the spectroscopic and electrochemical properties of the title dithiolene complexes, the M−S bond lengths were systematically overestimated. Subsequently, we reported relativistic TD-DFT calculations which highlighted how the trend in the metal−sulfur distances is affected by relativistic effects.[21,24] Now, in order to find the best level of theory to deal with adduct formation, new HF and DFT calculations with different basis sets and, in the case of DFT,

different functionals of the electron density, were performed on **10**−**12**, on I$_2$, and, for the sake of comparison, on Br$_2$ and IBr. The results of the calculations performed separately on **10**−**12** and on I$_2$ were used to find a suitable theoretical level to approach the donor−acceptor interaction leading to the model CT adducts **10**·I$_2$, **11**·I$_2$, and **12**·I$_2$. As regards DFT calculations, pure (BLYP[37,38] and BPW91[37,41]) and hybrid (mPW1PW[42] and B3LYP)[36−38] functionals were used. The PBE0 GGA functional[43] was not considered, since we have found recently that it gives results close to those obtained at the B3LYP level on the model dithiolene complexes **4** and **10**.[24] For all calculations, the Schafer, Horn and Ahlrichs pVDZ basis sets[44] were used for the organic framework, while for the central metal we tested the LanL2DZ,[39] SBKJC,[45] Stuttgart,[46] CRENBS[47] and CRENBL[47,48] basis sets with the corresponding effective core potential (ECP) sets. For halogens, the all-electron 6-311G**[49] and MIDI![50] and the sets LanL2DZ,[39] SBKJC,[45] and Stuttgart[46] with ECPs were used. Based on the results separately obtained on the interacting molecular units **10**−**12** and I$_2$,[51,52] the calculations on 1:1 adducts were performed on the model complexes **10**·I$_2$, **11**·I$_2$, and **12**·I$_2$ at the DFT level, using the mPW1PW functional and the LanL2DZ BSs with ECPs both for the central metal ion M and for iodine (see Supporting Information). A comparison between the optimised geometries of the adducts between **10**−**12** and I$_2$ shows a good agreement between the experimental bond lengths and angles reported previously[17,18] and those of the corresponding calculated values (Table 1). As an example, Figure 4 compares the bond lengths optimised for **11**·I$_2$ with those determined by X-ray diffraction[18] for **8**·I$_2$·CHCl$_3$.

Table 1. Optimised[a] bond lengths r (Å) and angles a (°) for the CT adducts **10**·I$_2$, **11**·I$_2$, and **12**·I$_2$, variations Δr (Å) and Δa (°) with respect to the free optimised[a] components and corresponding structural data r_{exp} (Å) and a_{exp} (°)[b] [c]

	10·I$_2$			**11**·I$_2$			**12**·I$_2$ [d]	
	$r_{\mathbf{10}\cdot I_2}$[a]	$\Delta r_{\mathbf{10}}$[a]	r_{exp}[b]	$r_{\mathbf{11}\cdot I_2}$[a]	$\Delta r_{\mathbf{11}}$[a]	r_{exp}[c]	$r_{\mathbf{12}\cdot I_2}$[a]	$\Delta r_{\mathbf{12}}$[a]
M−S(1,2)	2.186	−0.075	2.16	2.324	0.006	2.287	2.324	−0.004
M−S(1,2)[e]	2.193	−0.018	–	2.335	0.005	2.286	2.330	0.002
C(1,2)−S(1,2)	1.687	−0.003	1.70	1.700	0.006	1.697	1.701	0.006
C(1,2)−S(1,2)[e]	1.673	−0.017	–	1.685	−0.009	1.689	1.687	−0.008
C(1)−C(2)	1.399	−0.006	1.33	1.399	−0.007	1.343	1.396	−0.006
C(1)−C(2)[e]	1.418	0.013	–	1.418	0.012	1.403	1.413	0.011
C(3)−S(3)	1.669	0.024	1.68	1.675	0.030	1.740	1.676	0.031
C(3)−S(3)[e]	1.631	−0.014	–	1.639	−0.006	1.626	1.640	−0.005
S(3)−I(1)	2.855	–	2.83	2.918	–	2.875	2.918	–
I(1)−I(1)′	2.970	0.074	2.815	2.957	0.061	2.811	2.955	0.059
	$a_{\mathbf{10}\cdot I_2}$[a]	$\Delta a_{\mathbf{10}}$[a]	a_{exp}[b]	$a_{\mathbf{11}\cdot I_2}$[a]	$\Delta a_{\mathbf{11}}$[a]	a_{exp}[c]	$a_{\mathbf{12}\cdot I_2}$[a]	$\Delta a_{\mathbf{12}}$[a]
S(1)−M−S(2)	95.8	0.8	94.5	92.2	0.4	93.0	91.5	0.5
S(1)−M−S(2)[a]	94.8	−0.2	–	91.5	−0.3	92.1	90.7	−0.3
C(3)−S(3)−I(1)	95.9	–	97.4	96.4	–	98.3	96.2	–
S(3)−I(1)−I(1)′	179.6	–	177.5	180.0	–	179.6	179.9	–

[a] mPW1PW functional: Schafer et al. pVDZ BSs for C, H, N and S;[44] LanL2DZ with ECPs for Ni, Pd, and Pt.[39] [b] Average value from the X-ray crystal structure of **7**·2I$_2$·1/2I$_2$.[17] [c] Average value from the X-ray crystal structure of **8**·I$_2$·CHCl$_3$.[18] [d] No CT adduct containing any [Pt(R,R′timdt)$_2$] dithiolene complex has been structurally characterised to date. [e] Bond/angle in the non-interacting ligand.
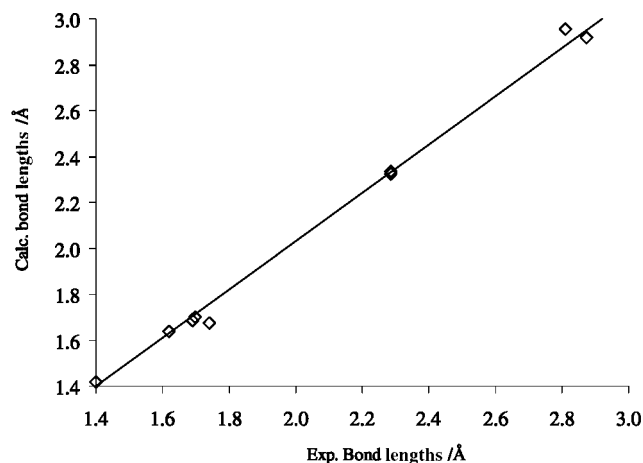
Figure 4. Bond lengths calculated for $11 \cdot I_2$ compared with the average structural bond lengths of $8 \cdot I_2 \cdot CHCl_3$ [18]

An interaction diagram (Figure 5 for $10 \cdot I_2$) between the molecular orbitals of the dithiolenes $10-12$ (D_{2h} point group) and those of molecular diiodine ($D_{\infty h}$ point group) shows that the Kohn–Sham HOMO and LUMO in the adducts, depicted in Figure 6 for $10 \cdot I_2$, derive from the σ-interaction of the b_{1u} HOMO and b_{2g} LUMO of the dithiolene with the $p\sigma_u^*$ LUMO of the I_2 molecule, whose energy is just intermediate between those of the two molecular orbitals of the complex. As expected from a qualitative fragment molecular orbital (FMO) interpretation of the donor–acceptor interaction,[53] the electron donation from the filled HOMO of the dithiolene to the antibonding LUMO of diiodine weakens the I–I bond. Due to the compositions of the HOMOs calculated for $10-12$, which are very similar in energy and do not contain significant contri-

butions from the central metals, the donor–acceptor interaction between [M(H2timdt)2] and iodine is not expected to be strongly dependent on M. In fact, the calculated lengthening in the I–I bond length of coordinated diiodine depends only slightly on the nature of the donor dithiolene complex (I–I: 2.830 Å for free I_2; 2.970, 2.957 and 2.955 Å in $10 \cdot I_2$, $11 \cdot I_2$, and $12 \cdot I_2$, respectively). The I–I elongation with respect to free I_2 is small (4.7%, 4.3%, and 4.2% for $10 \cdot I_2$, $11 \cdot I_2$, and $12 \cdot I_2$, respectively) in agreement with the structural results (3.6% and 3.5% for $7 \cdot 2I_2 \cdot 1/2I_2$, and $8 \cdot I_2$, respectively). As regards the metal dithiolene units, in agreement with the experimental results only very slight modifications are found in the metal–sulfur bond lengths compared to the optimised geometries of the dithiolenes $10-12$, which mainly regard the ligand unit interacting with the halogen (M–S = 2.189, 2.313, and 2.328 Å for **10**, **11**, and **12**, respectively, and 2.186, 2.324, and 2.324 Å for $10 \cdot I_2$, $11 \cdot I_2$, and $12 \cdot I_2$, respectively). An examination of all the other bond lengths within the dithiolene ligands shows that an intramolecular charge transfer is induced from the non-interacting H2timdt moiety to the interacting one, and then to the halogen molecule (intramolecular charge transfer). Thus, the non-interacting unit has a slightly higher trithione character than the interacting one (testified by a slight shortening of all C–S bond lengths, mainly in the terminal one, and a lengthening of the C–C bond length with respect to the other H2timdt ligand unit interacting with diiodine and to the free dithiolene). On the contrary, in agreement with the structures of $9 \cdot I_2$ and $8 \cdot I_2 \cdot CHCl_3$, the C–C bond lengths in the ligand unit interacting with iodine are calculated to be slightly shorter than in the free dithiolene. As expected, the terminal C(3)–S(3) bond interacting with diiodine is the most affected (1.637, 1.637, and 1.645 Å in
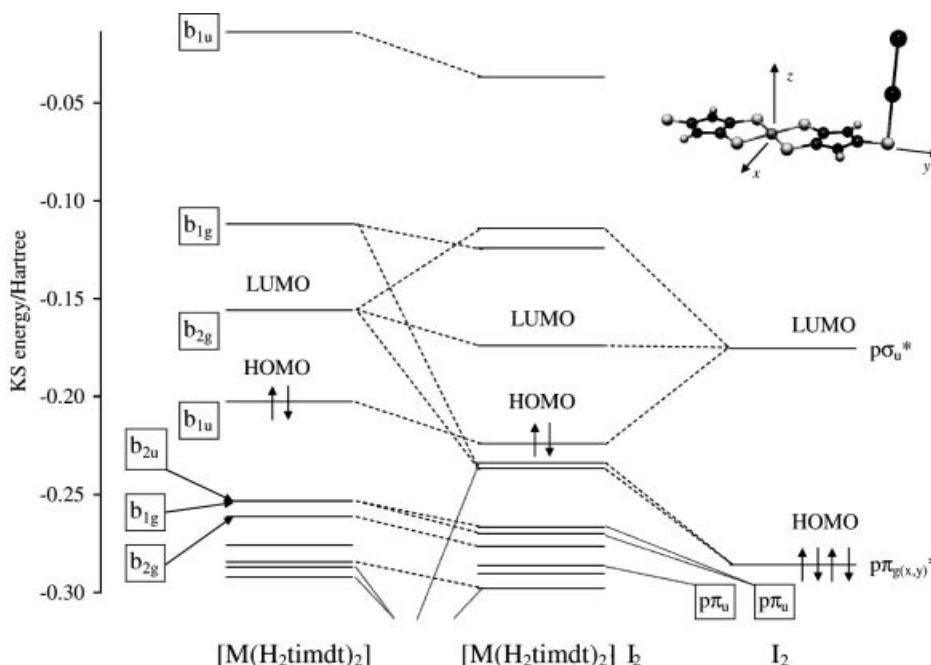

Figure 5. MO diagram showing the interaction between **10** and I_2; symmetry labels are referred to the D_{2h} space group (with the dithiolene on the xy plane) for **10** and $D_{\infty h}$ for I_2
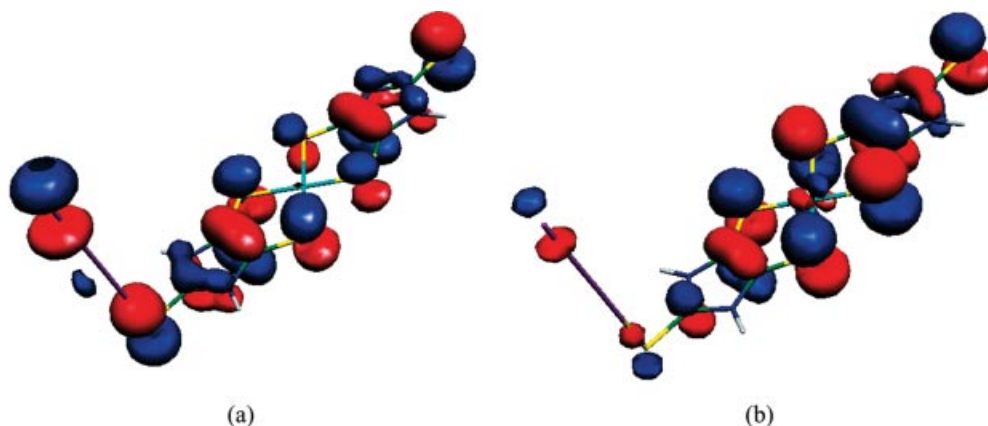
Figure 6. Drawings of Kohn−Sham HOMO (a) and LUMO (b) calculated for **10**·I_2

10, **11**, and **12**; 1.669, 1.675, and 1.676 Å in the interacting unit of **10**·I_2, **11**·I_2, and **12**·I_2, respectively). The strength of the interaction between the dithiolene donors and I_2 is reflected in the Wiberg bond indexes calculated for the involved groups. Thus, bond indexes of 0.287, 0.260, and 0.260 were calculated between the interacting terminal sulfurs and iodine in **10**·I_2, **11**·I_2, and **12**·I_2, respectively. Accordingly, the bond indexes of the interacting terminal thione groups (1.146, 1.391, and 1.388 for **10**·I_2, **11**·I_2, and **12**·I_2, respectively) are smaller than those of the free thione groups (1.639, 1.627, and 1.623 for **10**·I_2, **11**·I_2, and **12**·I_2, respectively), while the I−I bond order assumes fractional values in the three adducts (0.679, 0.702, and 0.704 for **10**·I_2, **11**·I_2, and **12**·I_2, respectively). The overall NBO-charge distribution in the three adducts (Table 2) confirms that the interaction between **10**−**12** and I_2 determines a charge transfer from the dithiolenes to the dihalogen, which depends only very slightly on the central metal ion, and is greater in the case of **10**·I_2 (charge on diiodine −0.295, −0.281, and −0.282 electrons for **10**·I_2, **11**·I_2, and **12**·I_2, respectively). In addition, the most negative charge in the adduct resides on the terminal iodine atom (−0.233, −0.212, and −0.213 for **10**·I_2, **11**·I_2, and **12**·I_2, respectively),

which is available for interacting with other iodine molecules. Accordingly, I−I···I−I contacts have been found in the crystal structures of **7**·2I_2·1/2I_2 and **8**·I_2·$CHCl_3$. This type of interaction could also account for the isolation of adducts having dithiolene/I_2 molar ratios higher than 1:2. The partial positive charge remaining on the dithiolene molecule is unevenly distributed over the two ligand units — the most positive being the non-interacting one — in agreement with the differences in the bond lengths described for the two ligands (the charge on the ligand interacting with diiodine is 0.130, 0.120, and 0.123 electrons and that on the non-interacting ligand is 0.166, 0.156, and 0.153 electrons for **10**·I_2, **11**·I_2, and **12**·I_2, respectively). Interestingly, the free terminal sulfur atom of the dithiolene carries a small residual negative charge, which allows for further interaction with a second diiodine molecule to give 1:2 adducts.

The coherent trends in the I−I bond lengths, in the charge transfer from the donor dithiolenes to iodine, and in the S−I and I−I bond indexes, calculated for **10**·I_2, **11**·I_2, and **12**·I_2, clearly indicate that the entity of the donor−acceptor interaction is almost constant on passing from **10**·I_2 to **12**·I_2, and is only slightly higher in the case

Table 2. NBO charge distribution[a] for compounds **4**−**6**, **10**−**12**, and the CT adducts **10**·I_2, **11**·I_2, and **12**·I_2

Atom	4	5	6	10	11	12	10·I_2	11·I_2	12·I_2
M	0.311	0.349	0.311	0.486	0.359	0.303	0.491	0.369	0.312
S(1)	0.037	0.067	0.086	−0.032	−0.003	0.015	0.130	0.120	0.123
S(1)′′[b]	−	−	−	−	−	−	0.010	0.002	0.005
C(1)	−0.391	−0.395	−0.400	−0.004	−0.007	−0.005	−0.008	−0.004	−0.009
C(1)′′[b]	−	−	−	−	−	−	0.006	0.009	0.003
N(1)/S[c]	0.493	0.492	0.490	−0.590	−0.589	−0.587	−0.569	−0.567	−0.567
N(1)′′[b]	−	−	−	−	−	−	−0.588	−0.583	−0.584
C(3)	−0.573	−0.573	−0.572	0.228	0.229	0.235	0.274	0.279	0.279
C(3)′′[b]	−	−	−	−	−	−	0.221	0.226	0.228
S(3)	0.069	0.069	0.063	−0.126	−0.127	−0.139	−0.087	−0.099	−0.105
S(3)′′[b]	−	−	−	−	−	−	−0.072	−0.078	−0.089
I(1)	−	−	−	−	−	−	−0.062	−0.069	−0.069
I[d]	−	−	−	−	−	−	−0.233	−0.212	−0.213

[a] Calculated at DFT/mPW1PW level. pVDZ basis set for C, H, N and S;[44] LanL2DZ with ECP for metal and halogen atoms.[39] Labelling scheme as in Figure 1. [b] For CT adducts, atom in the non-interacting ligand. [c] Endocyclic sulfur of the dmit ligand. [d] Terminal iodine atom.

of the nickel-dithiolene adduct. This is in agreement with the trend in the wavenumbers of FT-Raman-active stretching I−I frequencies measured for the adducts [M(Et₂timdt)₂]·2I₂. We therefore performed a calculation of the binding energy ΔE between **10** and I₂. In order to evaluate this energy, the renowned basis set superposition error (BSSE) has to be taken into account. This occurs when calculating the energy of an assembly of interacting monomers: each unit "borrows" Gaussian basis functions from the other components in order to describe its own electronic structure more accurately.[54] This results in an artificial overestimation of the interaction energies. Due to the computational effort required for these calculations, this correction has only been computed so far for small interacting systems, especially when geometrical deformations are to be taken into account.[54,55]

The BSSE in **10**·I₂ has been estimated by adapting the Boys−Bernardi full counterpoise (CP) correction scheme:[56]

ΔE_{BSSE} (**10**·I₂) = [E(**10**·I₂) − E_{fin}(**10**)^G − E_{fin}(I₂)^G] + [E_{str}(**10**) + E_{str}(I₂) − E(**10**) − E(I₂)] = [E(**10**·I₂) − E(**10**) − E(I₂)] + [E_{str}(**10**) + E_{str}(I₂)] − [E_{fin}(**10**)^G + E_{fin}(I₂)^G] = ΔE_{unc} + E_{str}(**10** + I₂) − E_{fin}(**10** + I₂)^G = ΔE_{unc} + $\delta\Delta E_{BSSE}$

so that the CP-corrected binding energy ΔE_{BSSE} is calculated from the uncorrected value ΔE_{unc} obtained from the total electronic energies calculated for **10**, I₂, and **10**·I₂ in their optimised geometries, [E(**10**), E(I₂) and E(**10**·I₂)], respectively], adding a BSSE correction term, $\delta\Delta E_{BSSE}$, calculated from the electronic energies computed for **10** and I₂ with [E_{fin}(**10** + I₂)^G = E_{fin}(**10**)^G + E_{fin}(I₂)^G] and without [E_{str}(**10** + I₂) = E_{str}(**10**) + E_{str}(I₂)], which are the "ghost" electronic functions of iodine and of the dithiolene atoms,

respectively, calculated at the "strained" equilibrium geometry assumed in the adduct. Finally, upon adding the Zero Point Energy (ZPE) correction, in order to account for the effects of molecular vibrations at 0 K, a CT-interaction energy $\Delta E_{ZPE,BSSE}$ of −10.94 kcal·mol^{-1} can be evaluated for **10**·I₂ (Table 3). It is worth noting that, since large basis sets are used for the organic framework and effective core potentials are used for the central metal and for the halogen atoms, the BSSE correction is small (1.235 kcal·mol^{-1}) compared to the CT-interaction energy. The calculated $\Delta E_{ZPE,BSSE}$ value confirms that the interaction between the dithiolene-complex donor and diiodine is weaker than those of similar systems, such as the CT adduct between imidazoline-2-thione and iodine (ΔE_{unc} = −18.554; $\delta\Delta E_{ZPE}$ = 0.860; $\delta\Delta E_{BSSE}$ = 1.477; $\Delta E_{ZPE,BSSE}$ = −16.216 kcal·mol^{-1}).

Table 3. Electronic energy (E) and electronic energy with ZPE correction (E_{ZPE}) for **10**, I₂, and **10**·I₂ (Hartree); electronic energy at the adduct geometry with (E_{fin}^G) and without (E_{str}) ghost electronic functions, calculated for **10** and I₂ (Hartree); uncorrected interaction energy ΔE_{unc}, ZPE correction $\delta\Delta E_{ZPE}$, BSSE correction $\delta\Delta E_{BSSE}$, and corrected CT-interaction energy $\Delta E_{ZPE,BSSE}$ for **10**·I₂ (mHartree and kcal mol^{-1})[a]

	E	E_{ZPE}	E_{str}	E_{fin}^G
10	−3007.6243	−3007.5068	−3007.6231	−3007.6244
I₂	−22.7951	−22.7947	−22.7925	−22.7932
10·I₂	−3030.4396	−3030.3209	−	−
	ΔE_{unc}	$\delta\Delta E_{ZPE}$	$\delta\Delta E_{BSSE}$	$\Delta E_{ZPE,BSSE}$
E (mHartree)	−20.197	0.800	1.968	−17.429
E (kcal·mol^{-1})	−12.674	0.502	1.235	−10.937

[a] mPW1PW functional: Schafer et al. pVDZ BSs for C, H, N and S;[44] LanL2DZ with ECPs for Ni, Pd, and Pt.[39]
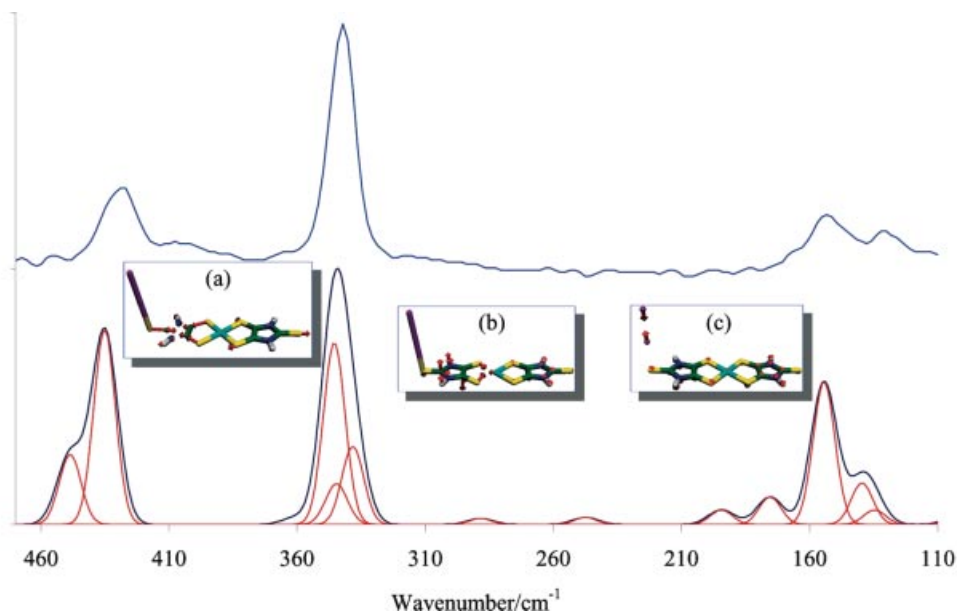

Figure 7. Normalised experimental FT-Raman spectrum recorded for **8**·2I₂ and simulated Raman spectrum of **11**·I₂ along with the constituent peaks in the range 110−450 cm^{-1}; insets the sketches of the normal harmonic vibrations responsible for the three main groups of bands

Finally, although the complete assignment of the Raman spectra recorded for the adducts between $[M(R,R'timdt)_2]$ and diiodine is beyond the scope of this work, the DFT calculations help us to understand the nature and type of the vibrational FT-Raman peaks. As described above, three groups of Raman peaks are found for all adducts in the far-IR region ($500-50$ cm^{-1}), although when using an FT-Raman spectrometer exploiting Nd:YAG lasers the lowest-energy peak can only rarely be observed experimentally because of the resonance Raman effect. As regards the two groups of peaks at higher wavenumbers (whose maxima for $10\cdot I_2$, $11\cdot I_2$, and $12\cdot I_2$ are calculated at 450, 508, and 438 cm^{-1} for the first group and 328, 345, and 372 cm^{-1} for the second, respectively), the calculated assignments do not differ from those previously reported for $10-12$.[17] Most importantly, the third group of peaks arises from the coupling between the I$-$I stretching and a waving vibration of the dithiolene complexes, resulting in two overlapping intense peaks, calculated at 146 and 156, 139 and 154, and 151 and 155 cm^{-1} for $10\cdot I_2$, $11\cdot I_2$, and $12\cdot I_2$, respectively. As an example, Figure 7 shows a comparison between the experimental FT-Raman spectrum recorded for $8\cdot 2I_2$ and the spectrum simulated for $11\cdot I_2$. In this case, the two overlapping peaks involving the I$-$I stretching vibration result in a single peak with a maximum at 155 cm^{-1}, in perfect agreement with the experimental values recorded for the adducts of $[Pd(Et_2timdt)_2]$.

Conclusions

The interaction between the neutral Ni, Pd, and Pt dithiolene complexes belonging to the general class $[M(R,R'timdt)_2]$ and diiodine has been investigated in depth from both an experimental and theoretical point of view. The donor ability of these dithiolenes, previously ascertained for Ni and Pd complexes, has now been confirmed also for Pt complexes. The characterisation of the reaction products has shown that different dithiolene/halogen molar ratios can be reached, depending on the nature of both the central metal ion and of the substituents R and R'. Among the synthesized adducts, $[Ni(Me,iPr\text{-}timdt)_2]\cdot I_2$ was characterised by X-ray diffraction on a single crystal, showing an unprecedented supramolecular network based on soft S···I interactions and due to the ability of diiodine to bridge different dithiolene stacks. A large set of preliminary calculations proved DFT to be more reliable than HFT in describing the structural and spectroscopic features of the model complexes $[M(H_2timdt)_2]$ (M = Ni, Pd, Pt) and of dihalogen and interhalogen molecules, such as I_2, Br_2, and IBr. The mPW1PW functional along with the LanL2DZ basis set adopted for the heaviest atoms have been used to investigate the model CT adducts $[M(H_2timdt)_2]\cdot I_2$. The computations are in very good agreement with structural and spectroscopic features. DFT calculations have shown that the soft-soft CT interaction involves σ-donation from the HOMO of the dithiolene donor to the LUMO of diiodine. In all cases, the DFT calculations

indicate that the title dithiolene complexes are medium-weak donors towards molecular iodine. In accordance with the composition of the Kohn−Sham HOMOs calculated for $[M(H_2timdt)_2]$, the I−I lengthening with respect to free I_2, the change in the Wiberg bond indexes, and the charge transfer calculated on the basis of the NBO-charge distribution, clarify that the donor ability of $[M(H_2timdt)_2]$ dithiolene complexes depends only marginally on the metal; it is only slightly higher in the case of M = Ni, in agreement with FT-Raman evidence. Thus, a binding energy of -10.83 kcal·mol^{-1} for the adduct $[Ni(H_2timdt)_2]\cdot I_2$ has been calculated from the electronic energies of the adduct and of the separated synthons, corrected both for ZPE and for BSSE according to the CP scheme.

Experimental Section

Materials and Methods: All solvents, reagents, and pressure tubes were purchased from Aldrich. All operations were carried out under a dry nitrogen atmosphere. The degree of purity of each compound was checked by CHNS and TLC analyses. Elemental analyses were performed on a FISONS EA-1108 CHNS-O instrument. Characterisation of all synthesized compounds was carried out as described previously.[17]

Synthesis of $[M(R,R'timdt)_2]\cdot nI_2$ Adducts: The dithiolene complexes $[M(R,R'timdt)_2]$ (M = Ni, Pd, Pt; R = R' = Et; R = Me, R' = iPr) were synthesised as reported previously.[18,19,23] They ($15-30$ mg) were then reacted with weighed amounts of diiodine in 1:1, 1:2, 1:5, and 1:10 molar ratios, in 30 mL of CHCl$_3$/hexane mixtures (1:3 v/v) according to the procedure described previously for the reaction between **8** and Br$_2$.[22] The stoichiometric ratios of the final products summarised in Scheme 1 were calculated on the basis of the elemental analyses.

$[Ni(Et_2timdt)_2]\cdot I_2$ (749.20): calcd. C 22.44, H 2.69, N 7.48, S 25.68; found C 21.53, H 2.39, N 6.54, S 24.92.

$[Ni(Et_2timdt)_2]\cdot 2I_2$ (1003.01): calcd. C 16.76, H 2.01, N 5.59, S 19.18; found C 17.12, H 1.95, N 5.06, S 19.09.

$[Ni(Et_2timdt)_2]\cdot 3I_2$ (1256.82): calcd. C 13.38, H 1.60, N 4.46, S 15.31; found C 13.46, H 1.24, N 4.41, S 14.69.

$[Pd(Et_2timdt)_2]\cdot 1/2I_2$ (670.02): calcd. C 25.10, H 3.01, N 8.36, S 28.71; found C 25.75, H 3.04, N 8.52, S 28.55.

$[Pd(Et_2timdt)_2]\cdot 2I_2$ (1050.74): calcd. C 14.76, H 1.77, N 4.92, S 16.88; found C 14.48, H 1.33, N 4.67, S 15.36.

$[Pt(Et_2timdt)_2]\cdot 2I_2$ (1139.40): calcd. C 14.76, H 1.77, N 4.92, S 16.88; found C 14.48, H 1.33, N 4.67, S 15.36.

$[Pt(Et_2timdt)_2]\cdot I_2$ (885.59): calcd. C 18.99, H 2.28, N 6.33, S 21.72; found C 18.19, H 1.79, N 6.40, S 21.18.

$[Pt(Et_2timdt)_2]\cdot 3/2I_2$ (1012.49): calcd. C 16.61, H 1.99, N 5.53, S 19.00; found C 16.70, H 1.82, N 5.50, S 19.20.

$[Ni(Me,iPr\text{-}timdt)_2]\cdot I_2$ (749.20): calcd. C 22.44, H 2.69, N 7.48, S 25.68; found C 22.54, H 2.56, N 7.47, S 24.68.

$[Ni(Me,iPr\text{-}timdt)_2]\cdot 4I_2$ (1519.63): calcd. C 11.13, H 1.33, N 3.71, S 12.73; found C 10.76, H 0.95, N 3.30, S 11.60.

$[Pd(Me,iPr\text{-}timdt)_2]\cdot 5/2I_2$ (1177.64): calcd. C 14.28, H 1.71, N 4.76, S 16.33; found C 14.79, H 1.47, N 4.80, S 16.99.

$[Pd(Me,iPr\text{-}timdt)_2]\cdot 2I_2$ (1050.74): calcd. C 16.00, H 1.92, N 5.33, S 18.31; found C 15.47, H 1.60, N 5.03, S 17.35.

$[Pt(Me,iPr\text{-}timdt)_2]\cdot 3I_2$ (1393.21): calcd. C 12.07, H 1.45, N 4.02, S 13.81; found C 12.48, H 1.15, N 3.68, S 13.67.

$[Pt(Me,iPr\text{-}timdt)_2]\cdot 4I_2$ (1647.02): calcd. C 10.21, H 1.22, N 3.40, S 11.68; found C 10.34, H 0.84, N 2.97, S 10.40.

[Pt(Me,*i*Pr-timdt)$_2$]·5I$_2$ (1900.82): calcd. C 8.85, H 1.06, N 2.95, S 10.12; found C 8.59, H 0.57, N 2.69, S 9.72.

Crystal Data for 9·I$_2$: C$_{14}$H$_{20}$I$_2$N$_4$NiS$_6$, triclinic, space group $P\bar{1}$ (no. 2), $a = 5.519(1)$, $b = 8.667(2)$, $c = 13.685(3)$ Å, $\alpha = 85.30(3)°$, $\beta = 80.34(3)°$, $\gamma = 72.70(3)°$, $U = 615.8(7)$ Å^3, $Z = 1$, $T = 293(2)$ K, $\mu = 38.12$ cm^{-1}. A needle crystal was mounted on a glass fiber in a random orientation on a Siemens SMART CCD area-detector diffractometer. Graphite monochromated Mo-K_α radiation ($\lambda = 0.71073$ Å) was used with the generator working at 45 kV and 40 mA. Cell parameters and orientation matrix were obtained from least-squares refinement on reflections measured in three different sets of 20 frames each in the range $0 < \theta < 28°$. 7082 Intensity data were collected in the full sphere (ω scan method), 2838 of which were unique. 2100 Frames (30 seconds per frame, $\Delta\omega = 0.3°$) were collected and the first 100 frames recollected to provide crystal decay monitoring, which was not observed. An absorption correction was applied using the SADABS routine.[57] The structure was solved by direct methods (SIR-97)[58] and refined on F^2 using the SHELX-97[59] program implemented in the WINGX suite.[60] Anisotropic displacement parameters were assigned to all non-hydrogen atoms. The hydrogen atoms were included in the structure model riding on their C atoms. The final values for $R1$ and $wR2$ were 0.041 and 0.084, respectively, for 1641 observed reflections [$I > 2\sigma(I)$] and 127 parameters. The maximum and minimum electron-density residual in the final ΔF map were 0.94 and -0.99 e·Å^{-3}, respectively. CCDC-224813 contains the supplementary crystallographic data for this paper. These data can be obtained free of charge at www.ccdc.cam.ac.uk/conts/retrieving.html [or from the Cambridge Crystallographic Data Centre, 12, Union Road, Cambridge CB2 1EZ, UK; Fax: +44 (0)1223 336033; E-mail: deposit@ccdc.cam.ac.uk].

Theoretical Calculations: Our aim was to compare the structures and energetics of model metal-dithiolene complexes **10**–**12**, iodine, and their CT adducts. Therefore, computations were carried out in such a way that the results could be compared reliably. Quantum chemical calculations were carried out on all compounds using the commercially available suite of programs Gaussian 98.[35] Although the use of all-electron basis sets provides better accuracy and efficiency, pseudopotential techniques are useful when relativistic effects have to be taken into account. Thus, the Schafer, Horn, and Ahlrichs all-electron pVDZ basis[44] was used for all calculations for C, N, and S. For Br and I the full-electron 6-311G**[49] and the MIDI![50] BS's, designed as a modification of the MIDI Huzinaga Split Valence basis,[61] and the LanL2DZ,[39] SBKJC,[45] and Stuttgart[46] BSs with effective core potentials (ECPs) were used.[62] For Ni, Pd, and Pt the LanL2DZ,[39] SBKJC,[45] Stuttgart,[46] CRENBS[47] and CRENBL[47,48] BSs were tested.[62] For DFT calculations on **10**–**12** and on the dihalogens Cl$_2$, Br$_2$ and I$_2$, the pure functionals BLYP,[34,36] BPW91[34,41] and the hybrid ones mPW1PW[42] and B3LYP[36–38] were tested. All geometry optimisations for complexes **10**–**12** were performed starting from the previously reported geometries (D_{2h} point group), computed with the B3LYP functional.[17] Due to a wrong default electronic initial guess, alteration of the initial ground state configurations of dithiolenes **10**–**12** (involving swapping of LUMO, HOMO, and HOMO−1) was needed in some cases. In particular, for HF calculations the "alter" option was used for **11** (SBKJC and Stuttgart BSs for Pd) and **12** (all BSs for Pt). For DFT calculations, the same problems were encountered when the functionals B3LYP (M = Ni, Pd, Pt with all BSs), BLYP (M = Pd with CRENBS, SBKJC and Stuttgart BS; Pt with all BSs), BPW91 (M = Pd with SBKJC BS; Pt with all BSs), and mPW1PW (M = Pd with SBKJC and

Stuttgart BSs; M = Pt with all BSs) were used. Interestingly, in the case of **10** and **11**, the removal of the inversion centre in the starting geometries allows the optimisation to converge to slightly lower energies. For the dithiolenes **4**–**6**, for the CT adducts **10·I$_2$**, **11·I$_2$**, and **12·I$_2$**, for imidazoline-2-thione, and for its 1:1 iodine adduct, DFT calculations were performed using the B3LYP and mPW1PW functionals and the LanL2DZ BS's with ECPs for the central metal ion and, if necessary, for halogen atoms. For all molecules, normal mode frequency calculations and NBO[63] charge distributions were calculated at the optimised geometries. The binding energies $\Delta E_{ZPE,BSSE}$, corrected for BSSE and ZPE, were calculated for the CT adducts between either **10** or imidazoline-2-thione and iodine as described above. All calculations were performed on an SGI Origin 3800 equipped with 128 Gb of RAM. The program Molekel 4.3 was used to investigate the shape of the calculated Kohn−Sham orbitals.[64] In order to simulate vibrational IR and Raman spectra starting from Gaussian output files, the program GaussFreq 2003[65] was developed using the RapidQ language. All spectra were simulated as superimposed Gaussian curves with a fixed halfband-width of 15 cm^{-1} starting from the calculated unscaled frequencies.

Supporting Information: Details on the criteria followed for choosing the computational level, calculated bond lengths and angles, and KS-orbital energies for dithiolenes **10**–**12**, bond lengths and normal mode frequencies of Br$_2$, I$_2$, and IBr have been deposited as Electronic Supporting Information (see also footnote on the first page of this article).

Acknowledgments

[1] G. N. Schrauzer, V. P. Mayweg, *J. Am. Chem. Soc.* **1965**, *87*, 3585−3592.

[2] U. T. Mueller-Westerhoff, B. Vance, D. Yoon, *Tetrahedron* **1991**, *47*, 909−932.

[3] L. J. Stewart, S. Bailey, B. Bennett, J. M. Charnock, C. D. Garner, A. S. McAlpine, *J. Mol. Biol.* **2000**, *299*, 595−602.

[4] B. S. Lim, J. P. Donahue, R. H. Holm, *Inorg. Chem.* **2000**, *39*, 263−273.

[5] K.-M. Sung, R. H. Holm, *Inorg. Chem.* **2000**, *39*, 1275−1281.

[6] C.-T. Chen, S.-Y. Liao, K.-J. Lin, L.-L. Lai, *Adv. Mater.* **1998**, *3*, 334−338.

[7] Z. Sun, M. Tong, H. Zeng, L. Ding, Z. Wang, Z. Xu, J. Dai, G. Bian, *Chem. Phys. Lett.* **2001**, *343*, 323−327.

[8] P. Cassoux, *Coord. Chem. Rev.* **1999**, *185-186*, 213−232. E. Canadell, *Coord. Chem. Rev.* **1999**, *185-186*, 629−651.

[9] B. S. Lim, D. V. Fomitchev, R. H. Holm, *Inorg. Chem.* **2001**, *40*, 4257−4262.

[10] M. D. Ward, J. A. McCleverty, *J. Chem. Soc., Dalton Trans.* **2002**, 275−288.

[11] R. Kimse, E. Möller, C. Seitz, J. Reinhold, *Z. Anorg. Allg. Chem.* **1997**, *623*, 159−168.

[12] W. E. Geiger, F. Barrière, R. J. LeSuer, S. Trupia, *Inorg. Chem.* **2001**, *40*, 2472−2473.

[13] K. W. Browall, T. Bursh, L. V. Interrante, *Inorg. Chem.* **1972**, *11*, 1800−1806. K. W. Browall, L. V. Interrante, *J. Coord. Chem.* **1973**, *3*, 27−38.

[14] Z. S. Herman, R. F. Kirchner, G. H. Loew, U. T. Mueller-Westerhoff, A. Nazzal, M. C. Zerner, *Inorg. Chem.* **1982**, *21*, 46−56.

[15] C. Lauterbach, J. Fabian, *Eur. J. Inorg. Chem.* **1999**, 1995−2004.

[16] F. Bigoli, P. Deplano, F. A. Devillanova, V. Lippolis, P. J. Lukes, M. L. Mercuri, M. A. Pellinghelli, E. F. Trogu, *J. Chem. Soc., Chem. Commun.* **1995**, 371−372.

[17] F. Bigoli, P. Deplano, F. A. Devillanova, J. R. Ferraro, V. Lippolis, P. J. Lukes, M. L. Mercuri, M. A. Pellinghelli, E. F. Trogu, J. M. Williams, *Inorg. Chem.* **1997**, *36*, 1218−1226.

[18] M. Arca, F. Demartin, F. A. Devillanova, A. Garau, F. Isaia, F. Lelj, V. Lippolis, S. Pedraglio, G. Verani, *J. Chem. Soc., Dalton Trans.* **1998**, 3731−3736.

[19] M. C. Aragoni, M. Arca, F. Demartin, F. A. Devillanova, A. Garau, F. Isaia, F. Lelj, V. Lippolis, G. Verani, *J. Am. Chem. Soc.* **1999**, *121*, 7098−7107.

[20] M. C. Aragoni, M. Arca, T. Cassano, C. Denotti, F. A. Devillanova, F. Isaia, V. Lippolis, D. Natali, L. Nitti, M. Sampietro, R. Tommasi, G. Verani, *Inorg. Chem. Commun.* **2002**, *5*, 869−872.

[21] T. Cassano, R. Tommasi, L. Nitti, M. C. Aragoni, M. Arca, C. Denotti, F. A. Devillanova, F. Isaia, V. Lippolis, F. Lelj, P. Romaniello, *J. Chem. Phys.* **2003**, *118*, 5995−6002. P. Romaniello, M. C. Aragoni, M. Arca, T. Cassano, C. Denotti, F. A. Devillanova, F. Isaia, F. Lelj, V. Lippolis, R. Tommasi, *J. Phys. Chem.* **2003**, *107*, 9679−9687.

[22] M. C. Aragoni, M. Arca, C. Denotti, F. A. Devillanova, E. Grigiotti, F. Isaia, F. Laschi, V. Lippolis, L. Pala, A. M. Z. Slawin, P. Zanello, J. D. Woollins, *Eur. J. Inorg. Chem.* **2003**, 1291−1295. M. C. Aragoni, M. Arca, F. A. Devillanova, F. Isaia, V. Lippolis, A. Mancini, L. Pala, A. M. Z. Slawin, J. D. Woollins, *Chem. Commun.* **2003**, 2226−2227.

[23] M. C. Aragoni, M. Arca, T. Cassano, C. Denotti, F. A. Devillanova, R. Frau, F. Isaia, F. Lelj, V. Lippolis, L. Nitti, P. Romaniello, R. Tommasi, G. Verani, *Eur. J. Inorg. Chem.* **2003**, 1939−1947.

[24] F. Lelj, P. Romaniello, M. Arca, F. A. Devillanova, *J. Phys. Chem.* **2003**, submitted.

[25] M. C. Aragoni, M. Arca, A. J. Blake, F. A. Devillanova, W.-W. du Mont, A. Garau, F. Isaia, V. Lippolis, G. Verani, C. Wilson, *Angew. Chem. Int. Ed.* **2001**, *40*, 4229−4232. M. C Aragoni, M. Arca, F. Demartin, F. A. Devillanova., A. Garau, F. Isaia, F. Lelj, V. Lippolis, G. Verani, *Chem. Eur. J.* **2001**, *7*, 3122−3133.

[26] M. C. Aragoni, M. Arca, F. A. Devillanova, A. Garau, F. Isaia, V. Lippolis, G. Verani, *Coord. Chem. Rev.* **1999**, *184*, 271−290.

[27] A. J. Blake, F. A. Devillanova, R. O. Gould, W.-S. Li, V. Lippolis, S. Parsons, C. Radek, M. Schröder, *Chem. Soc. Rev.* **1998**, *27*, 195−216.

[28] P. H. Svensson, L. Kloo, *Chem. Rev.* **2003**, *103*, 1649−1684.

[29] M. C. Aragoni, M. Arca, F. Demartin, F. A. Devillanova, A. Garau, F. Isaia, V. Lippolis, G. Verani, *Trends in, Inorg. Chem.* **1999**, *6*, 1−18.

[30] G. van Bolhius, P. B. Koster, T. Michelsen, *Acta Crystallogr.* **1967**, *23*, 90−91.

[31] P. Deplano, J. R. Ferraro, M. L. Mercuri, E. F. Trogu, *Coord. Chem. Rev.* **1999**, *188*, 71−95.

[32] The position of the peak due to the I−I stretching mode in the FT-Raman spectra of the CT adducts of [Ni(Et$_2$timdt)$_2$] is in agreement with the value (142 cm^{-1}) for $7 \cdot 2I_2 \cdot 1/2I_2$, reported in ref. 31.

[33] E. S. Kryachko, E. V. Ludeña, *Energy Density Function Theory of Many Electron Systems*, Kluwer Academic Publisher, **1990**, NL.

[34] B. Miehlich, A. Savin, H. Stoll, H. Preuss, *Chem. Phys. Lett.* **1989**, *157*, 200−206.

[35] *Gaussian 98* (Revision A.7), M. J. Frisch, G. W. Trucks, H. B. Schlegel, G. E. Scuseria, M. A. Robb, J. R. Cheeseman, V. G. Zakrzewski, J. A. Montgomery, R. E. Stratmann, J. C. Burant, S. Dapprich, J. M. Millam, A. D. Daniels, K. N. Kudin, M. C. Strain, O. Farkas, J. Tomasi, V. Barone, M. Cossi, R. Cammi, B. Mennucci, C. Pomelli, C. Adamo, S. Clifford, J. Ochterski, G. A. Petersson, P. Y. Ayala, Q. Cui, K. Morokuma, D. K. Malick, A. D. Rabuck, K. Raghavachari, J. B. Foresman, J. Cioslowski, J. V. Ortiz, B. B. Stefanov, G. Liu, A. Liashenko, P. Piskorz, I. Komaromi, R. Gomperts, R. L. Martin, D. J. Fox, T. Keith, M. A. Al-Laham, C. Y. Peng, A. Nanayakkara, C. Gonzalez, M. Challacombe, P. M. W. Gill, B. G. Johnson, W. Chen, M. W. Wong, J. L. Andres, M. Head-Gordon, E. S. Replogle, J. A. Pople, Gaussian, Inc., Pittsburgh, PA, **1998**.

[36] A. D. Becke, *J. Chem. Phys.* **1993**, *98*, 5648−5652.

[37] A. D. Becke, *Phys. Rev. A* **1988**, *38*, 3098−3100.

[38] C. Lee, W. Yang, R. G. Parr, *Phys. Rev. B* **1988**, *37*, 785−789.

[39] P. J. Hay, W. R. Wadt, *J. Chem. Phys.* **1985**, *82*, 270−283; *J. Chem. Phys.* **1985**, *82*, 284−298; *J. Chem. Phys.* **1985**, *82*, 299−310.

[40] D. P. Chong, O. V. Gritsenko, E. J. Baerends, *J. Chem. Phys.* **2002**, *116*, 1760−1772.

[41] K. Burke, J. P. Perdew, Y. Wang, in *Electronic Density Functional Theory: Recent Progress and New Directions* (Eds.: J. F. Dobson, G. Vignale, M. P. Das), Plenum Press, New York, **1998**.

[42] C. Adamo, V. Barone, *J. Chem. Phys.* **1998**, *108*, 664−675.

[43] J. P. Perdew, K. Burke, M. Ernzerhof, *J. Phys. Rev. Lett.* **1997**, *77*, 3865−3868.

[44] A. Schafer, H. Horn, R. Ahlrichs, *J. Chem. Phys.* **1992**, *97*, 2571−2577.

[45] W. J. Stevens, H. Basch, M. Krauss, *J. Chem. Phys.* **1984**, *81*, 6026−6033. W. J. Stevens, M. Krauss, H. Basch, P. G. Jasien, *Can. J. Chem.* **1992**, *70*, 612−630. T. R. Cundari, W. J. Stevens, *J. Chem. Phys.* **1993**, *98*, 5555−5565.

[46] P. Fuentealba, H. Preuss, H. Stoll, L. V. Szentpaly, *Chem. Phys. Lett.* **1982**, *89*, 418−422. A. Bergner, M. Dolg, W. Kuechle, H. Stoll, H. Preuss, *Mol. Phys.* **1993**, *80*, 1431−1441. P. Fuentealba, L. V. Szentpaly, H. Preuss, H. Stoll, *J. Phys. B* **1985**, *18*, 1287−1296. G. Igel-Mann, H. Stoll, H. Preuss, *Mol. Phys.* **1988**, *65*, 1321−1328. M. Dolg, U. Wedig, H. Stoll, H. Preuss, *J. Chem. Phys.* **1987**, *86*, 866−872. M. Dolg, H. Stoll, H. Preuss, R. M. Pitzer, *J. Phys. Chem.* **1993**, *97*, 5852−5859.

[47] L. A. LaJohn, P. A. Christiansen, R. B. Ross, T. Atashroo, W. C. Ermlen, *J. Chem. Phys.* **1987**, *87*, 2812−2824. R. B. Ross, J. M. Powers, T. Atashroo, W. C. Ermler, L. A. LaJohn, P. A. Christiansen, *J. Chem. Phys.* **1990**, *93*, 6654−6670.

[48] M. M. Hurley, L. F. Pacios, P. A. Christiansen, R. B. Ross, W. C. Ermler, *J. Chem. Phys.* **1986**, *84*, 6840−6853. W. C. Ermler, R. B. Ross, P. A. Christiansen, *Int. J. Quant. Chem.* **1991**, *40*, 829−846.

[49] L. A. Curtiss, M. P. McGrath, J-P. Blaudeau, N. E. Davis, R. C. Binning Jr., L. Radom, *J. Chem. Phys.* **1995**, *103*, 6104−6113. M. N. Glukhovtsev, A. Pross, M. P. McGrath, L. Radom, *J. Chem. Phys.* **1995**, *103*, 1878−1885.

[50] R. E. Easton, D. J. Giesen, A. Welch, C. J. Cramer, D. G. Truhlar, *Theor. Chim. Acta* **1996**, *93*, 281−301. J. Li, C. J. Cramer, D. G. Truhlar, *Theor. Chem. Acc.* **1998**, *99*, 192−196.

[51] It is worthy of note that the very narrow HOMO−LUMO gap classifies these dithiolene complexes as soft donors (Hardness = 0.674, 0.604, and 0.636 eV, for **10**, **11**, and **12**, respectively). In addition, the NBO charge distribution on **10−12** at the optimised geometries shows a negative charge on the terminal sulfur atoms. On the contrary, the charges on the terminal sulfur atoms of neutral dithiolenes **4−6**, calculated at the same level of theory, assume very small positive values. This difference in the charge distributions calculated in the two classes of complexes is in agreement with the donor ability towards halogens found for [M(R,R′timdt)$_2$] and never reported for dmit metal complexes.

[52] As expected on the basis of the HSAB theory, the hardness estimated from the HOMO and LUMO eigenvalues increases on passing from I$_2$ to Br$_2$ (hardness = 1.504, 1.625, and 1.760 eV for I$_2$, IBr, and Br$_2$, respectively, at mPW1PW/LanL2DZ level).

[53] I. Fleming, *Frontier Orbitals and Organic Chemical Reactions*, J. Wiley & Sons, New York, **1976**.

[54] F. F. Muguet, G. W. Robinson, *J. Chem. Phys.* **1995**, *102*, 3648−3654.

[55] A. Karpfner, *J. Phys. Chem. A* **2000**, *104*, 6871−6879.

[56] S. F. Boys, F. Bernardi, *Mol. Phys.* **1970**, *19*, 553−566.

[57] G. M. Sheldrick, SADABS, University of Göttingen, Germany, **1996**, to be published.

[58] A. Altomare, M. C. Burla, M. Camalli, G. L. Cascarano, C. Giacovazzo, A. Guagliardi, A. G. G. Moliterni, G. Polidori, R. Spagna, *J. Appl. Crystallogr.* **1999**, *32*, 115.

[59] G. M. Sheldrick, SHELX-97, *Program for Crystal Structure Refinement*, University of Göttingen, Germany, **1997**.

[60] L. J. Farrugia, *J. Appl. Crystallogr.* **1999**, *32*, 837.

[61] S. Huzinaga, J. Andzelm, M. Klobukowski, E. Radzio-Andzelm, Y. Sakai, H. Takewaki, *Gaussian Basis Sets for Molecular Calculations*, Elsevier, Amsterdam, **1984**.

[62] All BSs were obtained from the Extensible Computational Chemistry Environment Basis Set Database, Version 4/17/03, as developed and distributed by the Molecular Science Computing Facility, Environmental and Molecular Sciences Laboratory which is part of the Pacific Northwest Laboratory, P. O. Box 999, Richland, Washington 99352, USA, and funded by the U. S. Department of Energy. The Pacific Northwest Laboratory is a multi-program laboratory operated by Battelle Memorial Institute for the U. S. Department of Energy under contract DE-AC06-76RLO 1830. Contact David Feller or Karen Schuchardt for further information.

[63] NBO Version 3.1, E. D. Glendening, A. E. Reed, J. E. Carpenter, F. Weinhold.

[64] S. Portmann, H. P. Lüthi, *Chimia* **2000**, *54*, 766−769.

[65] Massimiliano Arca, GaussFreq 2003 for Windows, http://dipcia.unica.it/GaussFreq, **2003**.